Rank abundance relations in evolutionary dynamics of random replicators

Yoshimi Yoshino,[1,][*] Tobias Galla,[2,3,][†] and Kei Tokita[1,4,][‡]

[1]*Graduate School of Science and Cybermedia Center, Osaka University, Toyonaka, Osaka 560-0043, Japan*

[2]*The Abdus Salam International Centre for Theoretical Physics, Strada Costiera 11, 34014 Trieste, Italy*

[3]*The University of Manchester, School of Physics and Astronomy, Schuster Building, Manchester M13 9PL, United Kingdom*

[4]*Graduate School of Frontier Biosciences, Osaka University, Suita, Osaka 565-0871, Japan*

We present a nonequilibrium statistical mechanics description of rank abundance relations (RAR) in random community models of ecology. Specifically, we study a multispecies replicator system with quenched random interaction matrices. We here consider symmetric interactions as well as asymmetric and antisymmetric cases. RARs are obtained analytically via a generating functional analysis, describing fixed-point states of the system in terms of a small set of order parameters, and in dependence on the symmetry or otherwise of interactions and on the productivity of the community. Our work is an extension of Tokita [Phys. Rev. Lett. **93**, 178102 (2004)], where the case of symmetric interactions was considered within an equilibrium setup. The species abundance distribution in our model come out as truncated normal distributions or transformations thereof and, in some case, are similar to left-skewed distributions observed in ecology. We also discuss the interaction structure of the resulting food-web of stable species at stationarity, cases of heterogeneous cooperation pressures as well as effects of finite system size and of higher-order interactions.

　　　　PACS number(s): 87.23.Cc, 75.10.Nr, 31.15.xk

I. INTRODUCTION

Understanding the relationship between complexity and stability is a fundamental and controversial problem in ecology [1]. Before the 1970s the proposition that highly complex communities are more stable than simple ones was widely supported [2,3]. However, this early intuitive idea was challenged by theorists in the 1970s, who discussed the stability of a community of species interacting randomly [4]. In particular, the applications of random matrix theory rigorously revealed that the stability of a community strongly depends on complexity, e.g., diversity and statistical properties of the interaction matrix, such as variance and connectivity, and complexity tends to destabilize community dynamics [5]. Since then, many mathematical ecologists have studied random community models to explain the apparent contradiction between the complexity of real-world ecosystems and the results of these mathematical studies [6,7]. Recent theoretical developments, for example, have discovered stabilizing factors of random community models: competition [8] and antisymmetric prey-predator relationships [9]. Empirical and theoretical works also suggested importance of omnivory (higher connectance) [10,11] and weak interactions [12] for stability.

If the relative abundances of the species in a community are measured, inevitably a small number of very common species will be identified (i.e., species with a high abundance), along with some rare species and more numerous species of varying intermediate degrees of rareness. Clarifying the mechanisms underlying these rank abundance relations (RAR) (the relations between abundance and the number of species possessing that abundance) are clearly another fundamental problem of ecology [13,14]. In conservation biology as well, knowledge of RAR helps one to predict the likelihood of population persistence and community stability in face of global change. Various models have been applied to ecosystem communities [15–19] and, in special, the recent progress of the theory of "neutral" models [20–26] have aroused constructive discussions on theoretical predictions and the experimental studies on RAR. As the neutral models mainly cover ecosystem communities where species compete for niches on a single trophic level like a tropical forest or a coral reef, the models have left the more complex systems a mystery. Such systems occur on multiple trophic levels and include complex interactions, such as prey-predator relationships, mutualism, competition, and detritus food chains. Although RAR are observed universally in nature, their essential parameters have not been fully clarified.

As a step to explore RAR theoretically, in this paper, typical rank abundance relations are derived using a random community model with few parameters such as the level of symmetry of interaction matrix and cooperation pressure or productivity. While random community models can be criticized for a lack of immediate realism, they have the advantage of being exactly solvable by analytical techniques. Random replicator systems have, for example, been considered as solvable models of interacting species in Refs. [27–29]. In particlar, species abundance distributions of random replicator models with symmetric couplings have been computed in Ref. [29] using methods from equilibrium statistical mechanics. Such static approaches are limited to cases of symmetric couplings between species, in particular the presence of predator-prey pairs (for which interactions are highly asymmetric) can not be taken into account in such equilibrium approaches. In order to remedy these shortcomings, we here take a different dynamical approach, allowing for an extension to systems with an arbitrary proportion of predator-prey pairs. To this end we employ methods different from those of

*yoshimi@cp.cmc.osaka-u.ac.jp

†tobias.galla@manchester.ac.uk

‡tokita@cmc.osaka-u.ac.jp

Ref. [29] and focus on an approach based on dynamical generating functionals and path integrals.

It is interesting to note that stochastic models of complex dynamically assembled food-webs [30,31], which is from a simple dynamics governed by generalized birth and death events, derive reasonable species abundance distributions, in good agreement with real data. In such models the multispecies dynamics is effectively reduced to that of a representative species, subject to a "mean field" interaction with the remaining system. In a similar fashion our approach reduces the evolution of species randomly coupled via quenched interactions to a "one-species" effective process as well (albeit a non-Markovian one). This mapping leads to an exact solution in the thermodynamic limit of infinite system size. For the stochastic approach, the model has the randomness with some probability. On the other hand, for generation functional, it gives the fixed randomness in the deterministic time evolution. Apart from providing a starting point for more realistic modifications of the present model, our analysis can hence, to a certain degree, be seen as complementary to the approach of Refs. [30,31].

In the context of statistical mechanics another interesting point of the present model is that the replicator dynamics with asymmetric random interactions shows a nonequilibrium phase transition, i.e., two phases with qualitatively different behaviors are found (stable versus unstable). At the same time the replicator system does not exhibit a Lyapunov function, and is hence intrinsically a nonequilibrium model without detailed balance. Further details can be found in the statistical mechanics literature [32,33]. In our system destabilization of a globally fixed point solution and its bifurcation to limit cycle, heteroclinic cycle, and potentially chaos is found when parameters are varied. The random replicator model hence shows similarities, but also crucial differences compared with, e.g., models of spin glasses [34,35] and neural network models [36,37]. It is hoped that the study of random replicator dynamics may hence contribute to the understanding and classification of dynamical phase transitions in disordered systems.

This paper is organized as follows. We will define the model in Sec. II and then discuss the statistical mechanics analysis based on a path-integral approach in Sec. III. In Sec. IV, we show results for pairwise interaction: a stability analysis, phase diagram, survival function, rank-abundance relations (RAR), the species abundance distribution (SAD), finite size effects, and structure of the resulting food web are discussed. We then turn to heterogeneous cooperation pressure and higher-order interactions in Secs. V and VI, respectively. We summarize our results in Sec. VII.

II. MODEL

We here study the simplest system of random replicator subject to Gaussian interaction, and focus on the model originally proposed by Diederich and Opper [27,28]. In conventional replicator dynamics, the system consists of N species, labeled by $i=1,\ldots,N$. The composition of the population of species at time t is then described by a concentration vector $\mathbf{x}(t)=(x_1(t),\ldots,x_N(t))$, where $x_i(t)$ denotes the con-

centration of species $i=1,\ldots,N$, and where $\Sigma_i x_i(t)=1$. The system evolves in time according to the following replicator equations [38]

$$\frac{\dot{x}_i(t)}{x_i(t)} = f_i[\mathbf{x}(t)] - \nu(t), \qquad (1)$$

where $f_i[\mathbf{x}]$ is the "fitness" of species i at time t, and where $\nu(t)$ denotes the mean fitness of species in the population. Hence species fitter than average increase in concentration, whereas the weight of species less fit than average is reduced.

We here take the fitnesses $f_i[\mathbf{x}]$ to be frequency dependent, i.e., they are functions of the vector $\mathbf{x}$. Specifically we will assume, in the simplest setting, that

$$f_i[\mathbf{x}] = -2u x_i + \sum_{j \neq i} w_{ij} x_j, \qquad (2)$$

i.e., that interaction between species is pairwise and characterized by the matrix elements w_{ij}. Generalization to multispecies interaction is possible [39,40], and will be discussed below.

The matrix elements $\{w_{ij}, w_{ji}\}$ (for any pair $i < j$) are chosen from a Gaussian ensemble. Specifically we choose

$$\overline{w_{ij}} = 0, \quad \overline{w_{ij}^2} = \frac{w^2}{N}, \quad \overline{w_{ij} w_{ji}} = \Gamma \frac{w^2}{N}, \qquad (3)$$

where $\overline{\cdots}$ denotes an average over the random couplings. w here characterizes the magnitude of the interaction, and Γ is a symmetry parameter and takes values $\Gamma \in [-1,1]$. For $\Gamma = 1$ the interaction between any pair of species $i < j$ is fully symmetric, $w_{ij} = w_{ji}$. In this case no predator-prey pairs are found in the system. For $\Gamma = 0$ w_{ij} and w_{ji} are uncorrelated, the fraction of predator-prey pairs is hence 50%. For $\Gamma = -1$ all pairs of species are in predator-prey constellations, one here has $w_{ij} = -w_{ji}$. Choosing intermediate values of Γ allows one to interpolate smoothly between these regimes. The ecologically most relevant setup corresponds to negative values of Γ, describing prey-predator type interaction between species, rather than cooperation and direct mutual competition. Diagonal terms in Eq. (2) can be taken into account by writing $w_{ii} = -2u$, where u in the above setting denotes the so-called cooperation pressure [41]. In an ecological context u takes mostly positive values. For $u \to \infty$ the ecosystem is found in a state of perfect cooperation and maximal diversity (with all species surviving and having equal concentrations). The essential parameter $p = 2u$ can be termed as the productivity of a community in the sense of Lotka-Volterra equation (this will be explained in more detail in Sec. IV). Finally, in order to guarantee a well-defined thermodynamic limit $N \to \infty$, with which the statistical mechanics analysis of the model will be concerned, we rescale the concentration vector by a factor of N, and use the normalization $N^{-1}\Sigma_i x_i(t)=1$. Upon setting $\nu(t)=N^{-1}\Sigma_i x_i(t) f_i[\mathbf{x}(t)]$ this normalization is conserved by the replicator dynamics (1).

We will address the model by a combination of analytical and computational methods. The statistical mechanics theory is described in the following sections, and its results will be compared against simulations in the subsequent section. All

simulations are here performed using the method described in Ref. [42]. This numerical scheme effectively amounts to a first-order forward integration with a dynamically adapted time step. The latter is here necessary to avoid species concentrations to go negative in the discretized system. The dynamical time stepping used in our simulations if typically of the order of 0.01 to 0.1.

III. STATISTICAL MECHANICS THEORY

A. Path integral analysis

The above system can be addressed by generating functional techniques originally devised in the theory of disordered systems [43]. It is also applied to linear evolutionary dynamics model in Ref. [44] and can be adapted to the study of random Lotka-Volterra communities [45]. We will not detail the mathematical steps here, as they have been reported in depth in the literature [28,40]. In the thermodynamic limit the system is found to be described by an effective single-species process of the form [28]

$$\dot{x}(t) = x(t)\left(-2ux(t) - \Gamma \int_{t_0}^t dt'\, G(t,t')x(t') - \eta(t) - \nu(t) \right) \tag{4}$$

(t_0 denotes the time at which the dynamics is started). This process is non-Markovian in time, and subject to colored Gaussian noise $\eta(t)$, with temporal correlations given by

$$\langle \eta(t)\eta(t') \rangle = w^2 C(t,t'). \tag{5}$$

This colored noise is obtained from the interactions of randomness, which each trajectory has. $C(t,t')$ and $G(t,t')$ are the correlation and response functions, and are to be evaluated self-consistently as

$$C(t,t') = \langle x(t)x(t') \rangle_\star, \quad G(t,t') = \left\langle \frac{\delta x(t)}{\delta \nu(t')} \right\rangle_\star, \tag{6}$$

where $\langle \cdots \rangle_\star$ denotes an average over trajectories of the effective stochastic process (4). The analysis then proceeds by making a fixed-point ansatz, amounting to $Q \equiv C(t,t')$. We also write $\chi = \int dt\, G(t)$ for the integrated response, and consider only ergodic states in which χ remains finite. Restricting the analysis to asymptotically time-independent solutions of the effective process the following self-consistent equations for the resulting static order parameters Q, χ, and ν (the fixed-point value of the average fitness) can then be derived similar to those reported in Ref. [28]

$$\frac{M}{\sqrt{\lambda}} = \int_{-\infty}^{\Delta} Dz(\Delta - z), \tag{7}$$

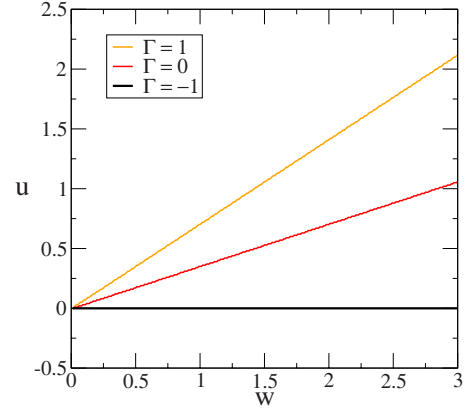$$\frac{QM^2}{\lambda} = \int_{-\infty}^{\Delta} Dz(\Delta - z)^2, \tag{8}$$

FIG. 1. (Color online) Phase diagram of the model with pairwise interaction in the (w,u) plane for $\Gamma = 1, 0, -1$ from top to bottom. The system approaches a unique stable fixed point in the region above the respective lines, and remains unstable and nonergodic below the phase boundaries.

$$-M\chi = \int_{-\infty}^{\Delta} Dz. \tag{9}$$

Here $Dz = \frac{1}{\sqrt{2\pi}} e^{-z^2/2} dz$ denotes the standard Gaussian measure, and one has $\lambda = w^2 Q$, $M = 2u + w^2\Gamma\chi$ and $\Delta = -\nu/\sqrt{\lambda}$. We note that $\phi = \int_{-\infty}^\Delta Dz = \frac{1}{2}[1 + \text{erf}(\Delta/\sqrt{2})]$ describes the fraction of surviving species. These equations are readily solved numerically, providing analytical predictions of the statistics of fixed-point solutions as functions of the model parameters w, Γ and u.

B. Cooperation pressure and strength of interaction

For reasons of completeness we re-iterate the phase behavior of the model as obtained by a linear stability analysis first reported in Ref. [28]. One here finds a stable region in which the fixed-point of the replicator dynamics is unique and locally attractive, separated from an unstable phase, as shown in Fig. 1.

For $\Gamma = -1$, the system is always found to be stable for any $u > 0$ independently of w. At fixed $w = 1$, the onset of instability occurs at $u_c = \sqrt{2}/4$ and $u_c = \sqrt{2}/2$ for $\Gamma = 0$ and $\Gamma = 1$, respectively. While the generating functional approach is applicable for general symmetry parameter Γ, a static analysis based on the replica method is possible for symmetric couplings ($\Gamma = 1$). This has been carried out in Refs. [27,46]. The replica approach is here fundamentally different from ours, as it is only of a static (time-independent) nature. The ergodic fixed-point phase corresponds to a regime in the static analysis in which only one well-defined minimum of the Lyapunov function is found, corresponding to a so-called replica symmetric solution [35]. This solution becomes unstable at the phase transition, referred to as a de Almeida-Thouless instability, coinciding with the location dynamical instability has been identified. For $u_c < u_c(\Gamma = 1, w = 1) = \sqrt{2}/2$ replica symmetry breaking (RSB) occurs, i.e., the manifold of minima of the Lyapunov function becomes disconnected [35]. In conclusion, while the replica approach, requiring the existence of a Lyapunov function, is limited to

the case $\Gamma = 1$, generating functionals can be used to study the replicator system for any degree of asymmetry in the interaction matrix, as this approach requires only the knowledge of the dynamical equations of the system (the replicator equations), but is independent of the existence or otherwise of a quantity minimized by these dynamics. For the case of symmetric couplings, $\Gamma = 1$, the results from both methods coincide. Finally, since the behavior of the system can be seen to be qualitatively independent of the coupling strength w (which effectively rescales the cooperation pressure), we will focus solely on $w = 1$ in the following.

C. Species abundance distribution (SAD)

Making a fixed point ansatz in the effective process (4) amounts to considering the time-independent solution of the effective species process of the form [28]

$$x(z) = \frac{-\nu - \sqrt{\lambda}z}{M}\Theta(-\nu - \sqrt{\lambda}z), \quad (10)$$

which represents the stochastic expression of the population in the stable state. z is here a static random variable drawn from a standard Gaussian distribution [$\sqrt{\lambda}z$ reflects the single-particle noise $\eta(t)$ which becomes time-independent in the fixed-point regime]. $\Theta(\cdots)$ is the step function. Note that, as mentioned above, only a fraction of species have positive concentrations at the fixed point, and that a complementary fraction of species dies out asymptotically. The distribution of concentrations x at the fixed point is thus a Gaussian cutoff at $x = 0$ combined with a δ-peak at $x = 0$ [42]. The so-called "survival function"

$$\alpha(x) = \lim_{N \to \infty} \frac{1}{N} \sum_i \overline{\Theta(x_i - x)}, \quad (11)$$

denotes the fraction of species with a concentration strictly larger than x at the fixed point. The survival function, indicating the probability of a species having an abundance larger than x, is easily computed from Eq. (10) and is found as

$$\alpha(x) = \frac{1}{2}\left[1 + \mathrm{erf}\left(\frac{\Delta - \frac{M}{\sqrt{\lambda}}x}{\sqrt{2}} \right) \right] \quad (12)$$

in the thermodynamic limit. The fraction of survivors ϕ as defined above is obtained as the special case $\phi = \alpha(x = 0)$.

Using the cumulative distribution function $C(x) \equiv 1 - \alpha(x)$ (denoting the probability for a species to have a concentration less than or equal to x) the abundance distribution for $x > 0$ is given by

$$F(x) = \frac{dC(x)}{dx} = \frac{M}{\sqrt{2\pi\lambda}} \exp\left(-\frac{\left(\Delta - \frac{M}{\sqrt{\lambda}}x \right)^2}{2} \right). \quad (13)$$

A similar expression has been obtained for the case of symmetric couplings ($\Gamma = 1$) based on replica techniques in Ref. [29]. These earlier findings are found from our generating
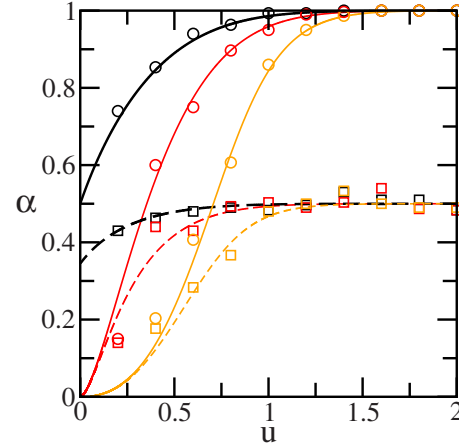

FIG. 2. (Color online) Survival functions $\alpha(0)$ and $\alpha(1)$ as functions of the cooperation pressure at fixed $w = 1$. Upper curves show $\alpha(0)$, lower curves $\alpha(1)$, with $\Gamma = -1, 0, 1$ from top to bottom in each group. Lines are from theory [valid only above $u_c(\Gamma)$], symbols from simulations of systems with $N = 300$ species, averaged over 20 samples. Surviving species in simulations are identified as species with $x_i > 0.01$ asymptotically.

functional analysis as a limiting case, so that generation functional analysis contains the technique of replica method as mentioned above.

IV. RESULTS FOR PAIRWISE INTERACTION

A. Survival function

We plot the survival functions $\alpha(x = 0)$ and $\alpha(x = 1)$ as a function of the cooperation pressure and for different values of Γ in Fig. 2. As seen in the figure the diversity of the population (as measured for example by the number of surviving species) increases with larger cooperation pressure. The figure also demonstrates good agreement between numerical simulations and theoretical predictions for large values of the cooperation pressure u. In this phase the system is stable and ergodic and hence the fixed-point theory applies. Numerical simulations are performed using the discretization scheme described in Ref. [42]. Below a critical value $u_c(\Gamma)$ stability and ergodicity are lost (for $\Gamma > -1$), and the above theory can no longer be expected to be accurate, and systematic deviations between theory and simulations may occur. Still the qualitative agreement between theoretical lines, extended into the unstable phase, where they are technically no longer valid, is surprisingly good (RSB effects have been seen to be weak in the low-u phase in previous studies). No unstable phase is present for fully anti-correlated couplings ($\Gamma = -1$) and non-negative cooperation pressure.

B. Rank-abundance relations

If the $S = \phi N$ surviving species are re-labeled and ordered according to their abundance in descending order, i.e., if $x_1 \geq x_2 \geq \cdots \geq x_S$ then $\alpha(x)$ can be understood as representing the species rank n according to
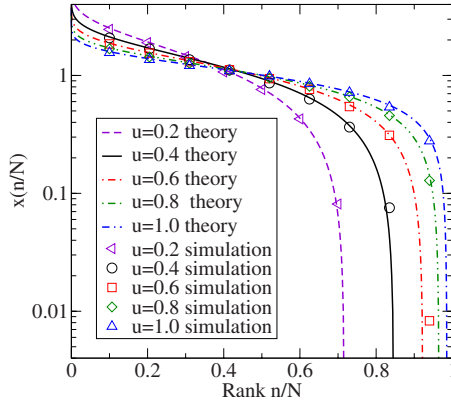
FIG. 3. (Color online) Rank abundance relation for $w=1$, $\Gamma=-1$. Markers are from simulations. ($N=200$, 20 samples, 10 000 iterations using the integration scheme of Ref. [42]), lines from the fixed point theory.

$$\alpha(x) = \frac{n}{N} \text{ for } x \in [x_{n+1}, x_n). \tag{14}$$

The function $\alpha(x)$ is a nonincreasing monotonic function, and can hence be inverted. The abundance $x(n/N)$ of the nth most abundant species can then be written as

$$x(n/N) = \alpha^{-1}(n/N). \tag{15}$$

This representation is generally referred to as a "rank abundance relations" (RAR) in the ecology literature. We find typical sigmoidal patterns which have been observed in different regions [20] and with different species compositions [47], see Figs. 3–5. In general, for large value of u the RAR are broad and corresponds to RAR for a species-rich community. Remarkably, the cross-over of the RAR patterns from low-to high-u is similar to the observed transition from low to high productivity areas in real-world data, that is, comparing species-poor areas such as an alpine or polar region to a species-rich tropical rain forest [20]. The transition also corresponds to the secular variation of patterns observed
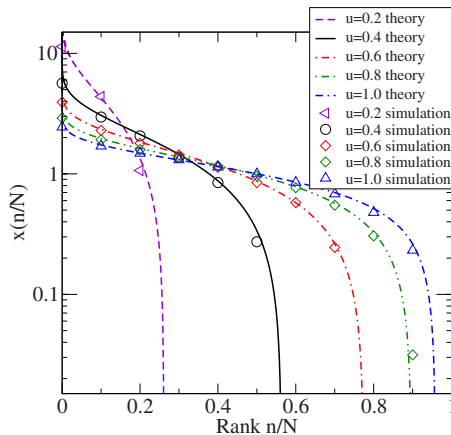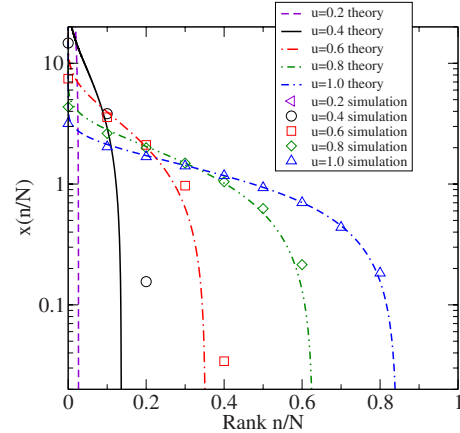

FIG. 4. (Color online) Rank abundance relation for $w=1$. $\Gamma=0$. Markers are from simulations. ($N=200$, 20 samples), lines from the fixed point theory, valid for $u>u_c=\sqrt{2}/4$, and of an approximate nature for $u<u_c$.

FIG. 5. (Color online) Rank abundance relation for $w=1$, $\Gamma=1$. Markers are from simulations. ($N=200$, 20 samples), lines from the fixed point theory, valid for $u>u_c=\sqrt{2}/2$, and of an approximate nature for $u<u_c$.

in abandoned cultivated land [48]. This supports the contention that u is a maturity parameter, as is suggested by an earlier evolutionary model in Ref. [49].

C. Species abundance distribution and Preston's octave plot

Empirical data of species abundance have been taken for example in the studies of Ref. [50–53], and are normally presented as plots of "species per octave." That is, species are grouped according to their abundance, and any species with abundance (number of individuals of that species present in the ecosystem) in the interval of say $[2^n, 2^{n+1})$ is subsumed in octave n (n being an integer). Log-normal distribution are then observed, e.g., in Refs. [51,52]. In order to depict the species abundance distributions in a manner similar to Preston's octave plot, we plot $xF(x)$ versus x in a log scale following Ref. [29], see Figs. 6–8 [64].

Generally, we find that an increased co-operation pressure (equivalently an increased productivity, see below) larger u leads to "octave plots" with small average and small variance. Species concentrations are here mostly found at a value
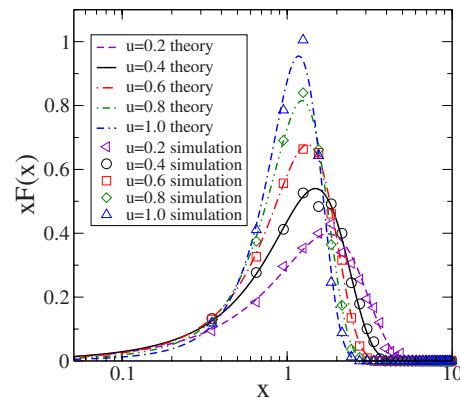

FIG. 6. (Color online) $\Gamma=-1$. The lines are from theory, $u=1.0, 0.8, 0.6, 0.4, 0.2$ from top to bottom. The stable phase extends to all $u>0$. Markers are from simulations. ($N=200$, averages over 50 samples are taken.)
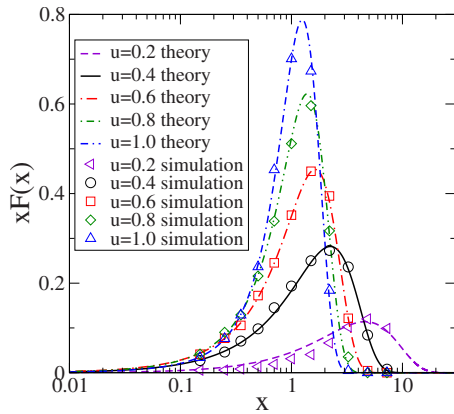
FIG. 7. (Color online) $\Gamma=0$. The lines are from theory, $u=1.0, 0.8, 0.6, 0.4, 0.2$ from top to bottom. Stable phase contains $u=1.0, 0.8, 0.6, 0.4$. $u=0.2$ is in the unstable phase where the theory applies only as an approximation ($u_c=\sqrt{2}/4$). Markers are from simulations. ($N=200$, 50 samples.)

FIG. 9. (Color online) $\Gamma=0$, $u=0.4$. The line is from theory, valid in the thermodynamic limit $N \to \infty$. Parameters are chosen such that the system is in the stable phase, but close to the transition point of the infinite system. Markers are from simulations, $N=10, 20, 50, 200$, respectively (averages over up to 10 000 samples are taken for small system sizes).

of around $x=1$ (in the limit of infinite cooperation pressure $u \to \infty$, all species have equal concentrations), and hence it is mostly the octave containing $x=1$ which is populated. On the other hand, for smaller u, fewer species survive, and the variance in their concentrations can be significant. This leads to octave plots of a large variance and a left-skewed form, similar to shapes observed, e.g., in Refs. [17,20]. In the fully asymmetric case $\Gamma=-1$, see Fig. 6 all theoretical curves are in good agreement with results from simulations for all values of u. Here the theory is exact. In Figs. 7 and 8, however, corresponding to $\Gamma=0$ and $\Gamma=1$ the theory is valid only for $u > u_c(\Gamma)$. Good agreement between analytics and simulations is again observed. For $u < u_c$ the theory is at best of an approximative nature, and data from simulations appears much more prone to noise, and systematic deviations are observed from theoretical lines if they are continued into the unstable phase. Qualitatively the theory is, however, able to capture the shape of the octave plots, in particular their left skewness.
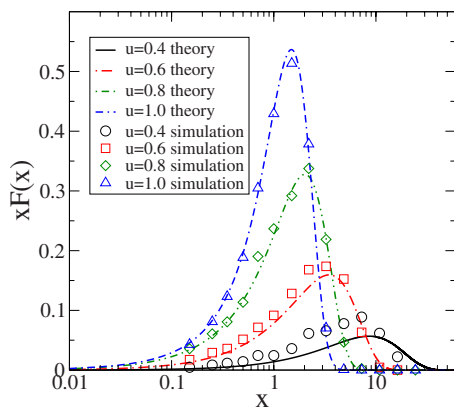
D. Finite size effects

Our theoretical analysis based on methods from statistical physics is mostly concerned with the limit of an infinite number of species in the ecosystem, $N \to \infty$. This is, of course, for analytical convenience only, but can be expected to be accurate also in the limit of large, but finite system size, as in real-world econetworks. To study deviations from the exactly tractable infinite-size limit we discuss simulation results of the species abundance distribution of small systems in Fig. 9. One realizes that the distribution becomes more left skewed as the system size N is reduced, and that systematic deviations from the theoretical lines emerge for systems smaller than about 100 species. For smaller N, the amplitude of the peak gets larger. Note also that the largest possible concentration is limited by N (due to the normalization $\sum_i x_i = N$), so that an effective upper cutoff is introduced for small systems, and the distribution is skewed to the left. In nature it is impossible to obtain data for species with an infinite concentration, so that the part of the curve at small

FIG. 8. (Color online) $\Gamma=1$. The lines are from theory, $u=1.0, 0.8, 0.6, 0.4$ from top to bottom. Stable phase $u=1.0, 0.8$ and unstable phase $u=0.6, 0.4$ ($u_c=\sqrt{2}/2$). Markers are from simulations. ($N=200$, 50 samples).
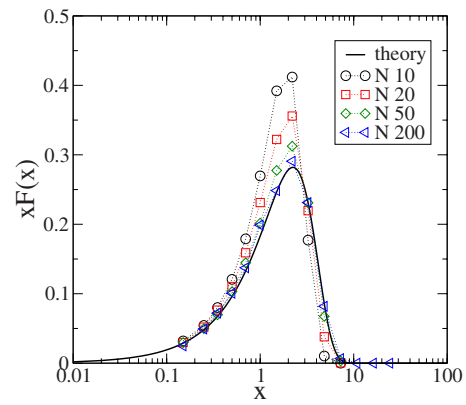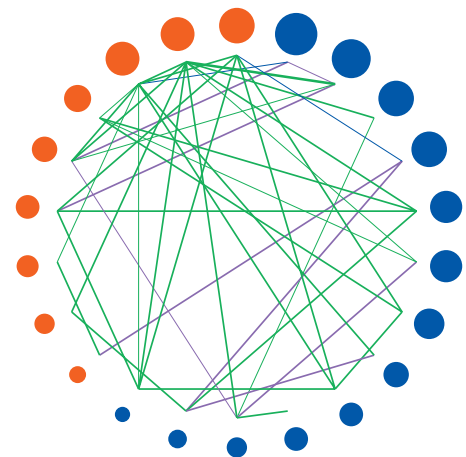

FIG. 10. (Color) Network of interspecies interactions for $w=1$, $\Gamma=1$, $N=100$, $u=0.4$.

TABLE I. Representation of the interspecies interactions as colored links. Species are assumed to be ordered such that $r_i > r_j$, for $i < j$.

Links	green	violet	blue	red
(b_{ij}, b_{ji})	$(+,+)$	$(-,-)$	$(+,-)$	$(-,+)$
interaction	mutual	competitive	i consumes j	j consumes i

and intermediate concentrations seems most relevant. Simulations indicate a trend toward more left skewness at small system sizes. Unlike in other models of statistical physics at or near their phase transition points, we are unable to see fat-tailed broad species abundance distributions in the present model.

E. Structure of the resulting food web

N-species replicator equations can in the context of ecology be shown to be equivalent to set of $N-1$ coupled Lotka-Volterra (LV) equations [38]. As discussed in Refs. [29,54] the following transformation of variables:

$$y_i = x_i / x_M \quad (i = 1, 2, \ldots, N), \tag{16}$$

$$r_i = w_{iM} - w_{MM} = w_{iM} + p, \tag{17}$$

$$b_{ij} = w_{ij} - w_{Mj} \tag{18}$$

renders the replicator system studied in the previous sections equivalent to Lotka-Volterra equations of the form

$$\frac{dy_i}{dt} = y_i \left(r_i - \sum_{j}^{N-1} b_{ij} y_j \right). \tag{19}$$

The "resource species" $M \in \{1, \ldots, N\}$ can here be chosen arbitrarily, note that one then has $y_M = 1$ by construction, leading to an $(N-1)$-dimensional system of LV equations. The ecological interspecies interactions b_{ij} are again of a Gaussian random form, but have different correlations than the couplings w_{ij} of the original replicator system. For $\Gamma = 1$ and $\Gamma = -1$, in particular, the b_{ij} need not carry the symmetry (antisymmetry, respectively, for $\Gamma = -1$) of the couplings w_{ij}. The LV model describes an interaction network of species, where the interaction between any given pair (i, j) of species $(i \neq j)$ can be of a mutualistic type (b_{ij} and b_{ji} both positive), of the competitive type (b_{ij} and b_{ji} both negative), or i and j can have a prey-predator relationship (one of the couplings positive, the other negative). These cases are summarized in Table I. The intraspecies interaction b_{ii} is given by $b_{ii} = w_{ii} - w_{Mi} = -p - w_{Mi} = -r_i$. r_i is here the intrinsic growth rate of species i in the LV equations, and follows a Gaussian distribution of mean p and variance $1/N$. In particular, in finite systems, r_i is positive with probability $\frac{1}{2}[1 + \text{erf}(\sqrt{N/2}p)]$. The parameter $p(=2u)$ can thus be interpreted as the "productivity" of the community (the larger p the more species have positive growth rate). Note also that the average growth rate $N^{-1}\Sigma_i \bar{r}_i$ is given by p.

In Figs. 10–12 we depict the food webs in the stationary
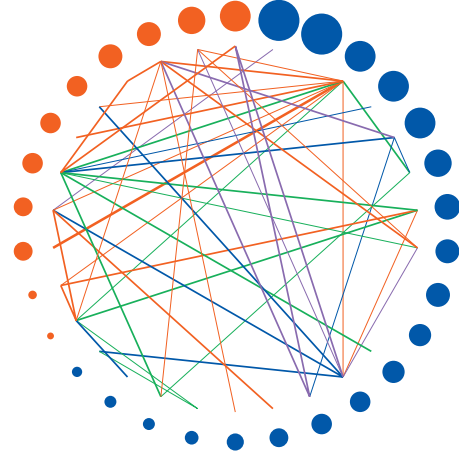

FIG. 11. (Color) Network of interspecies interactions for $w=1$, $\Gamma=0$, $N=100$, $u=0.2$.

state of the replicator (or equivalently LV) dynamics. Disks in these figures represent species, where species with a positive intrinsic growth rate ($r_i > 0$) are shown as blue disks, and species with negative growth rate are depicted as red disks. Upon ordering surviving species such that $r_1 \geq r_2 \geq \cdots \geq 0 \geq \cdots \geq r_S$, the radius of the disk representing species i is chosen to be proportional to $|\ln(r_1)|/|\ln|r_i||$. Note that the variance of interaction strengths scales as $1/N$ in our model, i.e., $w_{ij} \sim O(1/\sqrt{N})$, so for small u we can expect that $|r_i| < 1$ with large probability for any i (we have checked that $|r_i| < 1$ for all i for the data shown in Figs. 10–12). Since $|\ln|r_i||$ is monotonically decreasing function of $|r_i|$ in the interval $0 < |r_i| < 1$, larger blue disks hence mean larger productivity (i.e., fast growing species if interactions b_{ij} are switched off), and large red represent large antiproductivity (i.e., species with quickly decaying concentration in the absence of interactions in the LV system). Links between species are shown in the figures only if the effective interaction exceeds a certain threshold [i.e., if $\max(|b_{ij}|, |b_{ji}|) > 0.6 b_{max}$, where $b_{max} = \max(b_{ij}) \, \forall \, i, j$]. The thickness of each link in the figures is in proportion to $\max(|b_{ij}|, |b_{ji}|)$.

The different types of interactions (see Table I) are represented by different colors: green links denote mutualistic in-
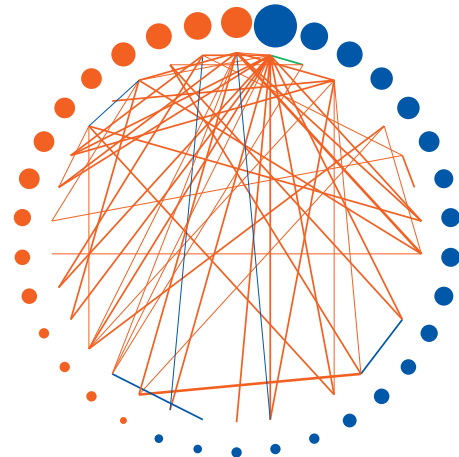

FIG. 12. (Color) Network of interspecies interactions for $w=1$, $\Gamma=-1$, $N=50$, $u=0.2$.

teractions, violet competitive interactions, blue lines denote cases where a more productive species i exploits a less productive one ($j > i$, assuming species are ordered such that $r_1 \geq r_2 \geq \ldots \geq r_S$), and red the reverse case of exploitation. In Fig. 10 we depict a resulting food web for the case of symmetric interactions ($\Gamma = 1$), no red links are observed in this case, as already reported in previous work [54]. On the other hand, one can see red links in Figs. 11 and 12. For $\Gamma = 1$ the interspecies relationships are hence almost all mutualistic, i.e., there are no prey-predator-type interactions in the equivalent Lotka-Volterra system. On the other hand, for $\Gamma = -1$ the relationships are almost all of the prey-predator type and mutualistic enhancing interactions are found only very rarely in the Lotka-Volterra system. The case of uncorrelated couplings in the replicator dynamics, $\Gamma = 0$, is an intermediate state. Finally, while we show the network topology only for small values of the cooperation pressure u in the figures, we note that with larger u, the network becomes more dense and of a more homogeneous structure.

V. SYSTEM WITH HETEROGENEOUS CO-OPERATION PRESSURE

Heterogeneity between species is in the present model represented by the random interactions w_{ij}. A second layer of diversity can be introduced, by making the cooperation pressure u species dependent, i.e., to use

$$f_i[\mathbf{x}] = -2u_i x_i + \sum_{j \neq i} w_{ij} x_j \tag{20}$$

as the fitness of species i, where now u_i carries an explicit index i and may be different from species to species. This model has been introduced and studied with generating functional techniques in Ref. [55]. In this section we will briefly discuss how adding heterogeneity of this type effects the distribution of surviving species, and will show how it can give rise to non-Gaussian abundance distributions and how these can be computed from the statistical mechanics theory. Specifically we will draw the $\{u_i\}$ from a flat distribution over an interval $[u_0 - \sigma, u_0 + \sigma]$, so that u_0 controls the mean co-operation pressure, and $\sigma \geq 0$ is variability over the ensemble of species. The generating functional analysis is straightforward, but leads to an ensemble of effective species processes, one for each cooperation pressure present in the population. A fixed-point ansatz then leads to coupled equations for the static order parameters Q, χ, Δ, expressed as integrals over the distribution of cooperation pressures, as reported in Ref. [55]. For $x > 0$ the distribution of concentration of surviving species is then found as

$$F(x) = \frac{1}{2\sigma} \int_{u_0 - \sigma}^{u_0 + \sigma} du \frac{M(u)}{\sqrt{2\pi\lambda}} \exp\left(-\frac{\left(\Delta - \frac{M(u)}{\sqrt{\lambda}} x\right)^2}{2}\right), \tag{21}$$

where $M(u) = 2u + w^2 \Gamma \chi$, $\lambda = w^2 Q$. This is a superposition of cutoff Gaussians, with varying mean and variances, and may hence for sufficient width σ of the distribution of cooperation
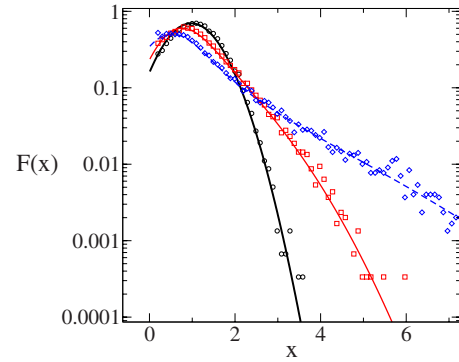

FIG. 13. (Color online) Linear-log plot of distribution $F(x)$ of surviving species for a system with heterogeneous cooperation pressures drawn from a flat distribution over $[1 - \sigma, 1 + \sigma]$, where $\sigma = 0.1, 0.5, 0.75$ from top to bottom at the maximum. Symbols are from simulations ($\Gamma = 0$, $w = 1$, $N = 300$ species, averages over 100 samples), solid lines from the generating functional fixed-point theory [note that for reasons of clarity we plot $F(x)$ not $xF(x)$ in contrast with other figures of previous sections].

pressures be of non-Gaussian shape. This is indeed observed in Fig. 13, where we depict $F(x)$ in a linear-log scale for various degrees of heterogeneity in the cooperation pressures. For small values of the width σ, the resulting function distribution $F(x)$ is relatively close to being Gaussian, but can develop slowly decaying tails, and nontrivial kurtosis if the cooperation pressures become sufficiently variable across species.

VI. HIGHER-ORDER INTERACTION

Up to now we have only considered the case of pairwise interaction between species. Generalization to higher-order interactions is possible and has been considered, for example, in Refs. [39,40]. A random community model with p-body interaction between species can be defined as follows:

$$\frac{d}{dt} x_i(t) = -x_i(t) \Bigg[2u x_i(t) + \sum_{(i_2, \ldots, i_p) \in M_i^{(p)}} J^i_{i_2, i_3, \ldots, i_p} x_{i_2}(t) x_{i_3}(t) \cdots x_{i_p}(t) - \nu(t) \Bigg], \tag{22}$$

with p a fixed integer and where $M_i^{(p)} = \{(i_2, \ldots, i_p) : 1 \leq i_2 < i_3 < \ldots < i_p \leq N; i_2, \ldots, i_p \neq i\}$. The coupling tensor is again assumed to be taken from Gaussian distribution with moments

$$\overline{(J^{i_1}_{i_2, \ldots, i_p})^2} = \frac{p!}{2N^{p-1}},$$

$$\overline{J^{i_1}_{i_2, \ldots, i_p} J^{i_k}_{i_1, \ldots, i_{k-1}, i_{k+1}, \ldots, i_p}} = \Gamma \frac{p!}{2N^{p-1}}. \tag{23}$$

We will consider $p = 3$ in the following. A generating functional and fixed-point analysis then leads to self-consistent equations
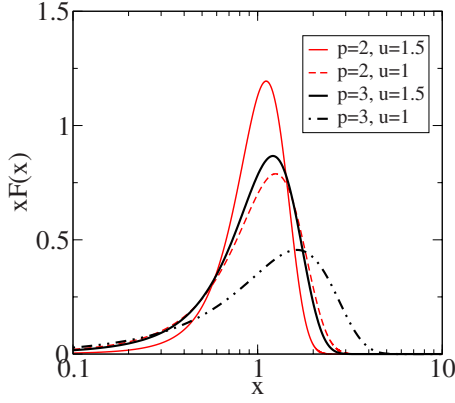
FIG. 14. (Color online) Abundance distribution $xF(x)$ for the system with two-species and three-species interaction. $\Gamma=0$, the cooperation pressure is set as in indicated in the legend.

$$\frac{M}{\sqrt{\lambda}} = \int_{-\infty}^{\Delta} Dz(\Delta - z), \qquad (24)$$

$$\frac{QM^2}{\lambda} = \int_{-\infty}^{\Delta} Dz(\Delta - z)^2, \qquad (25)$$

$$-M\chi = \int_{-\infty}^{\Delta} Dz, \qquad (26)$$

where $Dz = \frac{1}{\sqrt{2\pi}}e^{-z^2/2}dz$ again denotes the standard Gaussian measure. These equations are very similar to the ones derived above for the case $p=2$, differences are only to be found in the detailed expressions for the quantities M and λ, which now read $\lambda=\frac{3Q^2}{2}$, $M=2u+3\Gamma Q\chi$. We have $\Delta = -\nu/\sqrt{\lambda}$ as before.

Results for species abundance distribution of a replicator system with three-species interaction are depicted in Fig. 14 (for uncorrelated couplings, $\Gamma=0$), and compared to the case $p=2$ at otherwise unchanged parameters. For reasons of clarity we do not show results from numerical simulations, even though we have performed numerical tests in the ergodic stable phase and find reasonable agreement with the theoretical predictions. All other parameters kept equal, a three-body interaction appears to shift the peak of the distribution to the right, and to reduce its height, while increasing its width and left-skewness. Our findings thus suggest that higher-order interactions may add to the diversity of the ecological community, i.e., increase the variance of species concentrations at stationarity.

VII. SUMMARY AND CONCLUDING REMARKS

In summary we have presented a detailed discussion of species abundance relations resulting from the evolutionary dynamics of random replicator systems. Based on dynamical techniques of statistical mechanics of disordered systems we have extended the work of Refs. [29,54] to the case of asymmetric and antisymmetric coupling matrices, and have also taken into account higher-order interaction modes and sys-

tems in which species are subject to heterogeneous cooperation pressures. These systems typically show a phase transition between a stable, ergodic regime and an unstable phase, in which the final state of the system depends on initial conditions. Based on a fixed-point ansatz the statistical mechanics theory is able to deliver exact analytical predictions for the resulting species abundance relations in the limit of infinite system size, and computer simulations of the replicator dynamics are in perfect agreement with theoretical predictions. The key findings of our analysis are the following. (i) With larger cooperation pressure, regardless of interspecies interaction, the diversity of the population increases. (ii) We derive species-poor and species-rich RAR for symmetric interaction and species-rich RAR for asymmetric interaction. (iii) We find that the abundance distributions are typically similar to a lognormal distribution, and of a left-skewed type in our model, not too dissimilar from empirical data. (iv) Visualizing the food-web structure of surviving species, and distinguishing between different types of pairwise species interactions gives insight into the stable relationship between species at stationarity, in particular symmetric interactions favor mutualistic relations, whereas antisymmetric couplings tend to lead to one-sided exploitation of some species by others. (v) Survival functions of systems with heterogeneous cooperation pressure can display highly non-Gaussian survival functions with long tails. (vi) In finite systems our theory is not applicable, and systematic deviations are observed. In contrast with other disordered systems SAD are not found to be fat-tailed or skewed to the right near the transition of the infinite-size model.

The techniques we employ to study species abundance in random replicator systems are in the present context limited to fully connected random communities with Gaussian interactions. Extension to more realistic distributions of couplings may here be of interest, and similarly more realistic food-web topologies (see, e.g., Ref. [56] or [57], and references therein) could be taken into account in future work. Methods from disordered systems theory can be adapted to those cases as well, and further studies would most likely be based on cavity methods or other tools used for finite-connectivity disordered systems [58,59].

There is currently also much interest in the relationship between deterministic models of population dynamics (defined through rate equations, e.g., the above replicator dynamics) and stochastic individual-based models [60,61]. It has here been seen that demographic stochasticity in models with a finite-number of individuals can induce behavior quite different from models based on rate equations It may hence be of interest to investigate finite microscopic individual-based analogs of random replicator systems (for example, based on Moran dynamics) and to compare their dynamical behavior to that of the mean-field replicator system. Individual-based versions of systems with randomly drawn reaction rates have to our knowledge not been considered in the literature. This is indeed an interesting line of potential future work, although caution is appropriate when it comes to analytical approaches, as the randomness of interactions may make closed-form solutions of such models very difficult. It is hoped that our work may serve as a starting point for future studies in these directions, and that analysis of

random community models of theoretical ecology based on methods from statistical mechanics may hence contribute to an understanding of issues related to the diversity-stability debate as mentioned in the Introduction.

APPENDIX: GENERATING FUNCTIONAL ANALYSIS

The analysis of disordered systems by means of generating functional is a useful and powerful method, especially because it does not require the existence of a Lyapunov function, and is hence not limited to systems with symmetric interaction matrices. In this appendix we briefly outline the main mathematical steps and concepts of this technique. Further details can be found in a broad spectrum of sources in the literature [35,43,59,62].

The basic idea is to reduce a high-dimensional system with random couplings to an effective process for a representative (mean-field) particle. These processes are typically non-Markovian, even if the original system is Markovian, and subject to colored noise. If $\mathbf{x}(t) = (x_1(t), \ldots, x_N(t))$ represents a trajectory of the microscopic system (subject to random interactions), then the starting point of the analysis is the dynamical partition function (or generating functional)

$$Z[\psi] = \left\langle \exp\left[\sum_t i\psi(t)x_i(t) \right] \right\rangle, \quad \text{(A1)}$$

where $\langle \cdots \rangle$ represents an average over *all* possible trajectories of the system. The dynamic partition function can hence be expressed as a path integral over all such trajectories, and written in the form

$$Z[\psi] = \int D\mathbf{x}\,\delta(\text{equations of motion})e^{i\sum_t \psi(t)x_i(t)}. \quad \text{(A2)}$$

By "equations of motion" we here mean the microscopic equations governing the dynamics, in our case the replicator equations Eq. (1), they contain the quenched disorder of the problem (i.e., the random couplings). The analysis proceeds by writing the δ functions in their Fourier representation by means of conjugate variables $\{\hat{x}_i(t)\}$, subsequently performing the average over the disorder, and then by introducing suitable macroscopic order parameters, such as, e.g., the correlation function $C(t,t') = N^{-1}\sum_i x_i(t)x_i(t')$ and the response function $G(t,t') = iN^{-1}\sum_i x_i(t)\hat{x}_i(t)$. In the thermodynamic limit, $N \to \infty$, an effective theory for C and G is then derived, expressed as a self-consistent problem involving the above mentioned effective single-particle process in conjunction with self-consistent relations for correlation and response functions. As seen in Eqs. (4) and (5) the effective process makes reference to C and G, and, on the other hand, these order parameters are to be computed self-consistently as averages over the ensemble of effective-particle trajectories (6).

For general systems the effective single-particle problem can be addressed by suitable numerical schemes [63]. In the case of the replicator problem further analytical progress is possible based on the observation that the system attains a fixed point at sufficiently large cooperation pressure [28]. In this regime trajectories become effectively time-independent asymptotically, and further simplification is possible yielding Eqs. (7)–(9). Details of these steps can be found in Refs. [28,40].

[1] K. S. McCann, Nature (London) **405**, 228 (2000).

[2] R. H. MacArthur, Ecology **36**, 533 (1955).

[3] C. S. Elton, *The Ecology of Invasion by Animals and Plants* (Mathuen, London, 1958).

[4] M. R. Gardner and W. R. Ashby, Nature (London) **228**, 784 (1970).

[5] R. M. May, Nature (London) **238**, 413 (1972).

[6] R. M. May, *Stability and Complexity in Model Ecosystems*, 2nd ed. (Princeton University Press, Princeton, 1974).

[7] S. L. Pimm, *The Balance of Nature?* (Chicago University Press, Chicago, 1991).

[8] I. D. Rozdilsky and L. S. Stone, Ecol. Lett. **4**, 397 (2001).

[9] T. Chawanya and K. Tokita, J. Phys. Soc. Jpn. **71**, 429 (2002).

[10] S. P. Lawler and P. J. Morin, Am. Nat. **141**, 675 (1993).

[11] K. McCann, A. Hastings, and G. R. Huxel, Nature (London) **395**, 794 (1998).

[12] A.-M. Neutel, J. A. P. Heesterbeek, and P. C. de Ruiter, Science **296**, 1120 (2002).

[13] J. H. Brown, *Macroecology* (University of Chicago Press, Chicago, 1995).

[14] M. L. Rosenzweig, *Species Diversity in Space and Time* (Cambridge University Press, Cambridge, 1995).

[15] R. M. May, In *Ecology and Evolution of Communities*, edited by M. L. Cody and J. M. Diamond (Belknap, New York, 1975), pp. 81–120.

[16] G. Sugihara, Am. Nat. **116**, 770 (1980).

[17] S. Nee, P. H. Harvey, and R. M. May, Proc. R. Soc. London, Ser. B **243**, 161 (1991).

[18] M. Tokeshi, *Species Coexistence* (Blackwell, London, 1998).

[19] M. Hall, K. Christensen, S. A. di Collobiano, and H. J. Jensen, Phys. Rev. E **66**, 011904 (2002).

[20] S. P. Hubbell, *The Unified Neutral Theory of Biodiversity and Biogeography* (Princeton University Press, Princeton, 2001).

[21] I. Volkov, J. R. Banavar, S. P. Hubbel, and A. Maritan, Nature

(London) **424**, 1035 (2003).

[22] R. S. Etienne and H. Olff, Ecol. Lett. **7**, 170 (2004).

[23] D. Alonso and A. J. McKane, Ecol. Lett. **7**, 901 (2004).

[24] R. S. Etienne, Ecol. Lett. **8**, 253 (2005).

[25] D. Alonso, R. S. Etienne, and A. J. McKane, Trends Ecol. Evol. **21**, 451 (2006).

[26] R. S. Etienne and D. Alonso, J. Stat. Phys. **128**, 485 (2007).

[27] S. Diederich and M. Opper, Phys. Rev. A **39**, 4333 (1989).

[28] M. Opper and S. Diederich, Phys. Rev. Lett. **69**, 1616 (1992).

[29] K. Tokita, Phys. Rev. Lett. **93**, 178102 (2004).

[30] A. J. McKane, D. Alonso, and R. V. Solé, Phys. Rev. E **62**, 8466 (2000).

[31] R. V. Solé, D. Alonso, and A. J. McKane, Philos. Trans. R. Soc. London, Ser. B **357**, 667 (2002).

[32] G. F. Mazenko, *Nonequilibrium Statistical Mechanics* (Wiley-VCH, Weinheim, 2006).

[33] R. K. Pathria, *Statistical Mechanics* (Butterworth-Heinemann, Oxford, 1996).

[34] D. Sherrington and S. Kirkpatrick, Phys. Rev. Lett. **35**, 1792 (1975).

[35] M. Mezard, G. Parisi, and A. Virasoro, *Spin Glass Theory and Beyond* (World Scientific, Singapore, 1987).

[36] A. Düring, A. C. C. Coolen, and D. Sherrington, J. Phys. A **31**, 8607 (1998).

[37] K. Mimura, M. Kawamura, and M. Okada, J. Phys. A **37**, 6437 (2004).

[38] J. Hofbauer and K. Sigmund, *The Theory of Evolution and Dynamical Systems* (Cambridge University Press, Cambridge, 1988).

[39] V. M. de Oliveira and J. F. Fontanari, Phys. Rev. Lett. **85**, 4984 (2000).

[40] T. Galla, J. Phys. A **39**, 3853 (2006).

[41] M. Peschel and W. Mende, *The Prey-Predator Model* (Springer-Verlag, Vienna, 1986).

[42] M. Opper and S. Diederich, Comput. Phys. Commun. **121-122**, 141 (1999).

[43] C. De Dominicis, Phys. Rev. B **18**, 4913 (1978).

[44] H. Rieger, J. Phys. A **22**, 3447 (1989).

[45] T. Galla (unpublished).

[46] P. Biscari and G. Parisi, J. Phys. A **28**, 4697 (1995).

[47] R. H. Whittaker, *Communities and Ecosystems* (Macmillan, New York, 1970).

[48] F. A. Bazzaz, Ecology **56**, 485 (1975).

[49] K. Tokita and A. Yasutomi, Theor Popul. Biol. **63**, 131 (2003).

[50] R. A. Fisher, A. S. Corbet, and C. B. Williams, J. Anim. Ecol. **12**, 42 (1943).

[51] F. W. Preston, Ecology **43**, 185 (1962).

[52] F. W. Preston, Ecology **43**, 410 (1962).

[53] R. H. MacArthur, Proc. Natl. Acad. Sci. U.S.A. **43**, 293 (1957).

[54] K. Tokita, Ecol. Inf. **1**, 315 (2006).

[55] T. Galla, e-print arXiv:0711.0169.

[56] S. N. Dorogovtsev and J. F. F. Mendes, *Evolution of Networks: From Biological Nets to the Internet and WWW* (Oxford University Press, Oxford, 2003).

[57] J. A. Dunne, R. J. Williams, and N. D. Martinez, Proc. Natl. Acad. Sci. U.S.A. **99**, 12917 (2002).

[58] A. K. Hartmann and M. Weigt, *Phase Transitions in Combinatorial Optimisation Problems* (Wiley-VCH, New York, 2005).

[59] A. C. C. Coolen, N. S. Skantzos, I. Perez Castillo, C. J. Perez Vicente, J. P. L. Hatchett, B. Wemmenhove, and T. Nikoletopoulos, J. Phys. A **38**, 8289 (2005).

[60] A. J. McKane and T. J. Newman, Phys. Rev. E **70**, 041902 (2004).

[61] A. J. McKane and T. J. Newman, Phys. Rev. Lett. **94**, 218102 (2005).

[62] A. C. C. Coolen, *Handbook of Biological Physics* edited by F. Moss and S. Gielen (Elsevier, Amsterdam, 2000).

[63] H. Eissfeller and M. Opper, Phys. Rev. Lett. **68**, 2094 (1992).

[64] We here note that upon writing $\omega_i = \ln(x_i)$ for the octave to which a species with concentration $x_i > 0$ belongs, and $G(\omega)$ for the "density of species" per octave ω, one has $\int_\omega^{\omega+1} G(\omega') d\omega' = \int_{e^\omega}^{e^{\omega+1}} F(x) dx$, so that one realizes by substitution that $G(\omega) = e^\omega F(e^\omega) = x F(x)$, which motivates our plotting of $xF(x)$ in a log-linear scale. Note that for convenience we do not use a base of two in this context, but choose natural logarithms instead. This amounts to no more than an overall rescaling by a constant factor.